

Forces in molecules

Jesús Hernández-Trujillo,^a Fernando Cortés-Guzmán,^a
De-Chai Fang^b and Richard F. W. Bader^{*b}

Received 7th April 2006, Accepted 1st June 2006

First published as an Advance Article on the web 19th September 2006

DOI: 10.1039/b604996f

Chemistry is determined by the electrostatic forces acting within a collection of nuclei and electrons. The attraction of the nuclei for the electrons is the only attractive force in a molecule and is the force responsible for the bonding between atoms. This is the attractive force acting on the electrons in the Ehrenfest force and on the nuclei in the Feynman force, one that is countered by the repulsion between the electrons in the former and by the repulsion between the nuclei in the latter. The virial theorem relates these forces to the energy changes resulting from interactions between atoms. All bonding, as signified by the presence of a bond path, has a common origin in terms of the mechanics determined by the Ehrenfest, Feynman and virial theorems. This paper is concerned in particular with the mechanics of interaction encountered in what are classically described as ‘nonbonded interactions’—are atoms that ‘touch’ bonded or repelling one another?

1. Introduction

1.1 Forces determining atomic interactions

The quantum averaging of the momentum operators— $\hbar\nabla$ for an electron and for a nucleus transforms the electrostatic Hamiltonian into the forces that act on the electrons and on the nuclei, the Ehrenfest force and the Feynman force, respectively. These are the only forces operative in a field-free molecular system. The molecular virial theorem relates the virial of the Ehrenfest force acting on the electrons to their kinetic energy, the molecular virial including a contribution from the virial of the Feynman forces acting on the nuclei.¹ *Thus through the Ehrenfest and Feynman theorems, one has the tools that are needed to describe the forces acting in a molecule and, through the virial theorem, to relate these forces to the molecule's energy and its kinetic and potential contributions in the manner promulgated by Slater.*²

1.2 Nonbonded interactions

The study of the behaviour of both the Ehrenfest force (EF) and Feynman force (FF) as a function of internuclear separation, as is performed in this paper, is important for the understanding of atomic interactions, from long-range attractions to the supposed presence of ‘nonbonded’ interactions encountered upon close-approach. ‘Nonbonded interactions’ between atoms, particularly ‘nonbonded repulsions’ is a model frequently invoked in discussions of both intramolecular and intermolecular interactions. The correct physical description in a given situation is essential to understanding the structures of molecules and crystals.³ Ascribing

^a Facultad de Química, Universidad Nacional Autónoma de México D. F., 04510 México

^b Department of Chemistry, McMaster University, Hamilton, Ontario, Canada, L8S 4M1

barriers that are believed to arise from nonbonded interactions to 'Pauli or exchange repulsions'⁴ or hyperconjugative electron release⁵ is carried out by invoking the properties of non-existent states, a step that removes one from physics and any comparison with experiment, an unnecessary step in any event when the underlying physics is in reality uncomplicated.⁶ It is demonstrated here that the repulsion that does exist between atoms upon close approach is a consequence of just one force, the nuclear–nuclear electrostatic force of the Feynman theorem.

Bonding is ubiquitous and so is its representation in terms of bond paths, including situations that clearly lie beyond the applicability of simplified orbital models.⁷ The existence of condensed phases of matter and of intra-molecular clusters, as simple as hydrogen bonding or the bound states of diatomic rare gas molecules, all fall under the heading of closed-shell interactions and thus lie beyond the scope of zeroth-order orbital electron pair model of bonding. One is struck by the dichotomy of existing interpretations of nonbonded interactions: two atoms that touch (that is, approach to within their van der Waals radii) can in certain cases be said to repel one another, a repulsion frequently ascribed to 'steric or Pauli repulsions', or to be bonded to one another to yield molecular clusters or condensed states. How does one decide whether two atoms that 'touch' are bonded or are repelling one another? Physics of course, provides an answer to this question and it is this answer that forms the basis of this paper.

The necessary physics is provided by the quantum theory of atoms in molecules (QTAIM). QTAIM determines which atoms 'touch' in any system regardless of the nature of the interaction, by the presence of a (3,–1) critical point in the density. Its presence indicates that the atoms share an interatomic surface—the definition of 'touch'—and are linked by an atomic interaction line. If the Feynman forces on the nuclei of the atoms vanish or are attractive, the line is termed a bond path.

2. From forces to energies in molecular formation

The paper is concerned primarily with a discussion of the interdependence of the Ehrenfest and Feynman forces with the total energy and its potential and kinetic components, from the neighbourhood of the equilibrium separations down to the UA limit, that is, for $R \leq R_e$. QTAIM relates the mechanics of bonding between atoms in any system to a study of the individual interactions wherein each is defined by an interatomic surface and by a line of maximum density linking their nuclei which in an equilibrium geometry is a bond path. The analysis is applied to the N_2 , CO, LiF and He_2 diatomic molecules, representative of shared, polar, ionic and van der Waals bonding because nonbonded interactions will in general, incur all possible interactions. The information obtained in the study of the atomic interactions in the diatomic molecules, as summarized by the surface and atomic properties obtained from QTAIM, is readily extended to interactions with similar characteristics in a polyatomic system.

2.1 Calculations

All wave functions were calculated using large basis sets at the QCISD level of theory⁸ and subject to satisfaction of the virial theorem using self consistent virial scaling (SCVS)⁹: cc-pV5Z for He_2 with the *g* basis function removed, cc-pVTZ for N_2 and CO all from Woon and Dunning¹⁰ and the basis set given by the contraction (10s,6p,4d)/[5s,2p,2d] of Sadlej and Urban for LiF.^{11,12} The tendency of the maxima in ρ at nuclear positions, as described by a GTO basis, to migrate off-nucleus into the bonding region upon close-approach was countered by including s and p basis functions with exponents of 50 000 and 1000, respectively. Their inclusion in the basis set used in He_2 for example, reduced the displacement from 1×10^{-2} au to 9×10^{-4} for $R = 0.5$ au and from 2×10^{-2} to 2×10^{-3} au for $R = 0.08$ au.

2.2 Ehrenfest and Feynman forces

The EF acting on the electronic charge contained in some infinitesimal volume element, $\rho(\mathbf{r})d\tau$, is the net result of its attraction by all of the nuclei and its repulsion by the average distribution of the remaining electrons. The Feynman force (FF) on a nucleus on the other hand, is the resultant of the attraction of the nucleus by the electronic charge in each volume element $\rho(\mathbf{r})d\tau$ and its repulsion by the remaining nuclei.¹³ Both forces operate in real space and have electrostatic interpretations.

The Ehrenfest force density, $\mathcal{F}(\mathbf{r})$, the force exerted on the electron density at some point in space, is defined in eqn (1) in terms of the gradient of the total potential energy operator \hat{V} with respect to the coordinates of one electron. Its averaging, in the identical procedure used to define the electron density, that is, averaging over the motions of all the electrons other than electron '1' as denoted by $\int d\tau'$, followed by multiplication by N , yields the Ehrenfest force density,

$$\mathcal{F}(\mathbf{r}) N \int d\tau' \psi^*(-\nabla_1 \hat{V})\psi \quad (1)$$

$\mathcal{F}(\mathbf{r})$ is N times the force exerted on an electron at position \mathbf{r} by the *average distribution* of the remaining electrons and by the rigid nuclear framework—the force exerted on the electron density.

An atom in a molecule is an open system bounded by its zero-flux surface^{14,15} and the force acting on all of the electrons in the atom, the Ehrenfest force $\mathcal{F}(\mathbf{A})$, is equal and opposite to the force exerted on its surface, eqn (2).

$$\mathcal{F}(\mathbf{A}) = \int_{\mathbf{A}} d\mathbf{r} \mathcal{F}(\mathbf{r}) = - \int_{\mathbf{A}} d\mathbf{r} \nabla \cdot \boldsymbol{\sigma}(\mathbf{r}) = - \oint d\mathbf{S}(\mathbf{r}; \mathbf{A}) \cdot \boldsymbol{\sigma}(\mathbf{r}) \quad (2)$$

It may be expressed in terms of an integral of the Ehrenfest force density or alternatively, in terms of the divergence of the stress tensor,^{14,16} enabling $\mathcal{F}(\mathbf{A})$ to be transformed into a surface integral *via* Gauss' theorem. The stress tensor has the dimensions of pressure—of force per unit area—and thus the stress tensor determines the force exerted on each element of the atomic surface and its product with an element of the surface $d\mathbf{S}(\mathbf{r})$, as in eqn (1), gives the force acting on that element.¹⁷ An atomic surface $\mathbf{S}(\mathbf{r}; \mathbf{A})$ is in general, composed of a number of separate interatomic surfaces, there being one such surface associated with each bond path terminating at the \mathbf{A} nucleus. In this account, $\mathcal{F}(\mathbf{A})$ will refer to the force acting across a single interatomic surface. In the case of a diatomic, this equals the total force on either of the atoms, but in the general case of a polyatomic system, $\mathcal{F}(\mathbf{A})$ will refer to the force acting between the two groups defined by the surface. $\mathcal{F}(\mathbf{A})$ can be attractive, drawing two atoms or groups together towards the interatomic surface, or repulsive, tending to draw both away from the surface.¹⁶ The atomic forces are necessarily equal and opposite and no net force acts on an atom or group or on any element of density in a stationary state, but the direction of EF is important in determining the mechanics of atomic interactions.

The behaviour of EF as a function of internuclear separation has been shown to be characteristic for interactions extending from shared to closed-shell,¹⁶ its behaviour in CO shown in Fig. 1 being representative. It is repulsive for large separations, attaining a maximum value in the region of the inflexion point in the molecule's potential energy curve, the point where the Feynman force on a nucleus is maximally attractive. Upon closer approach, the EF decreases, changing sign for a separation in excess of R_e and becoming increasingly attractive. This is the result of the continued accumulation of density in the binding region between the nuclei. The attraction of the nucleus external to \mathbf{A} for the density of \mathbf{A} , is the principal stabilizing force in the formation of a molecule and its virial is the principal source of energy lowering.^{16,18} In general, the single largest contribution to $\mathcal{F}(\mathbf{A})$, the force on atom \mathbf{A} in a diatomic \mathbf{AB} in the vicinity of R_e , is the attraction of the \mathbf{B} nucleus for the density on \mathbf{A} and the largest single contribution to the lowering of the energy is the potential energy of

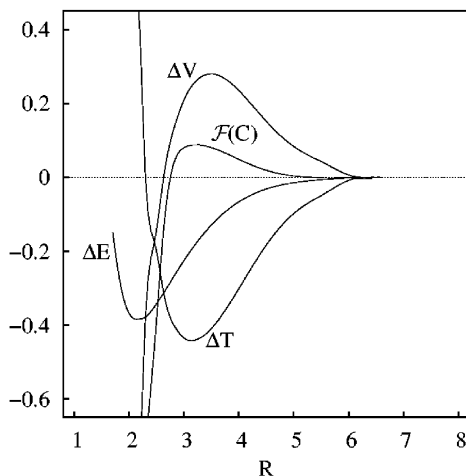


Fig. 1 Variation of ΔE , ΔT , ΔV and $\mathcal{F}(C)$ the Ehrenfest force on the carbon atom, with $\mathcal{F}(C) = -\mathcal{F}(O)$, for the formation of CO from ground state atoms, from a multi-reference CI calculation using a large basis set.¹⁹ Energy and distance scales are in atomic units in all diagrams. The depicted behaviour is universal, applying to homopolar, polar and van der Waals interactions. Even an ionic interaction such as LiF exhibits an initial decrease in T and increase in V for large R before the onset of charge transfer causes their behaviour to be dominated by the Feynman force, $\mathcal{F}(R)$, as occurs at ~ 10 au for LiF.

interaction of the nucleus of one atom interacting with the density of the other.¹⁸ In the case of a polyatomic system, the interatomic surface determining EF and its properties are characteristic of the nature of the interaction between the atoms sharing the surface. This is the anticipated result, as QTAIM has the important property of reflecting the principal observations of chemistry: that an atom exhibits characteristic properties with respect to one interaction, even when linked to different neighbours. There are many documented examples of this behaviour, a necessary consequence of QTAIM recovering the observed properties of atoms in molecules. Thus the properties of a surface are characteristic for a particular interaction. As a case in point, consider the Ehrenfest force acting on the C1|C2 surface in adamantane before and after the insertion of a Be^{+2} ion into the cage. The Be^{+2} is bonded to the four methine C1 atoms and represents a major perturbation of the system. Nonetheless, the magnitude of the force acting in the C1|C2 surface, which is attractive, changes by only 0.02 au from 0.11 au to 0.13 au upon insertion. The properties of the C–H and C–C bond critical points caused by the insertion of a number of neutral and charged atoms leave the characterization of the surface in terms of these properties unchanged.¹⁶

2.3 The virial theorem

The force density can be converted into a potential energy density by forming the ‘virial of the force operator—the force acting through a distance’, by taking its scalar product with the position vector \mathbf{r} to yield

$$\nu^0(\mathbf{r}) = \mathbf{r} \cdot \mathcal{F}(\mathbf{r}) = N \int d\tau' \psi^* (-\mathbf{r} \cdot \nabla \hat{V}) \psi \quad (3)$$

$\nu^0(\mathbf{r})$ defines a potential energy of interaction of the electron density at some position \mathbf{r} . If one integrates $\nu^0(\mathbf{r})$ over all space it yields the virial ν , the virial of all the forces acting on the density, as defined in eqn (4)

$$\nu = V_{\text{en}} + V_{\text{ee}} - \sum_{\alpha} \mathbf{X}_{\alpha} \cdot \mathbf{F}_{\alpha\text{e}} \quad (4)$$

The molecular virial ν equals the electron–nuclear V_{en} , and electron–electron V_{ee} potential energies together with the sum $\sum_{\alpha} \mathbf{X}_{\alpha} \cdot \mathbf{F}_{\alpha\text{e}}$, the virial of the electronic contribution to the Feynman forces exerted on the nuclei, \mathbf{X}_{α} being the coordinate of nucleus α . \mathbf{F}_{α} , the Feynman force on nucleus α , equals the sum of the electronic and nuclear forces, $\mathbf{F}_{\alpha} = \mathbf{F}_{\alpha\text{e}} + \mathbf{F}_{\alpha\text{n}}$, and one may replace $\mathbf{F}_{\alpha\text{e}}$ with $\mathbf{F}_{\alpha} - \mathbf{F}_{\alpha\text{n}}$ in eqn (4) to recast the nuclear virial into the contribution from the sum of the virials of the Feynman forces exerted on the nuclei, $\mathbf{X}_{\alpha} \cdot \mathbf{F}_{\alpha}$, and the nuclear–nuclear repulsion energy $V_{\text{nn}} = \sum_{\alpha} \mathbf{X}_{\alpha} \cdot \mathbf{F}_{\alpha\text{n}}$. Thus the molecular virial ν , obtained by averaging the virial of the Ehrenfest force acting on the electron density, equals the total potential energy V plus the virial of the Feynman forces on the nuclei,¹⁴

$$\nu = V_{\text{en}} + V_{\text{ee}} + V_{\text{nn}} - \sum_{\alpha} \mathbf{X}_{\alpha} \cdot \mathbf{F}_{\alpha} = V - \sum_{\alpha} \mathbf{X}_{\alpha} \cdot \mathbf{F}_{\alpha} \quad (5)$$

The molecular virial theorem relates T , the kinetic energy of the electrons to the virial of the Ehrenfest forces acting on them,

$$2T = -\nu \quad (6)$$

For a diatomic molecule, the virial of the Feynman force, the term $\sum_{\alpha} \mathbf{X}_{\alpha} \cdot \mathbf{F}_{\alpha}$ becomes $RF(R)$ and the theorem takes the form

$$2T = -V - R(dE/dR) = -V + RF(R) \quad (7)$$

The virial theorem inter-relates the kinetic and potential energies of the electrons with the virial of the Feynman forces acting on the nuclei, all as a function of R . For $R = \infty$ and for the equilibrium separation, $F(R)$ vanishes and one obtains the result $2T = -V$ or equivalently, since $E = T + V$, $T = -E$. The same relationships hold for the separated atoms and defining the difference between the energy for the molecular minus the separated atom values by Δ , one obtains the well-known constraints on the energy changes accompanying the formation of a bound state for which $\Delta E < 0$: $\Delta E = \frac{1}{2}V$ and $\Delta E = -\Delta T$ at $R = R_{\text{e}}$. Thus molecular stability is a result of a decrease in the potential energy that necessarily requires an increase in the kinetic energy. This interpretation is consistent with the requirement of the electrostatic theorem of bonding, that electronic charge be accumulated in the bonding region, since next to the nuclear positions, the internuclear region exerts the lowest potential. Thus the virial and electrostatic theorems give mutually consistent interpretations of chemical bonding, an anticipated result since, as pointed out by Slater “...both the virial theorem and Feynman’s theorem are exact consequences of wave mechanics.”²

The variations in E , T and V over the range of R up to R_{e} are given for H_2^+ and H_2 by Slater² and for LiF , N_2 , CO and Ar_2 by Bader and Hernández-Trujillo.¹⁹ The behaviour shown for CO in Fig. 1 is general for the approach of neutral atoms. One may combine the virial and Feynman theorems, through the use of eqn (7), to obtain differential statements for $dT(R)$ and $dV(R)$. These expressions yield constraints on the signs of the slopes $dT(R)/dR$ and $dV(R)/dR$ which are seen from Fig. 1 to change sign with decreasing R . The derivation of these equations and their full discussion are given elsewhere,^{14,20} their consequences being summarized here. For large values of R lying in the range $\infty > R > R_1$ (the inflection point in attractive arm of $E(R)$, Fig. 1), the signs of the derivatives are not uniquely determined, being the result of the two competing contributions, $F(R)$ and $RdF(R)/dR$, being of opposite sign. However, for the approach of neutral atoms at large values of R , $RdF(R)/dR$ will dominate with the result that T must decrease and V increase upon the initial approach of two neutral atoms (or the approach of one neutral and one charged atom). These changes are understandable in terms of the accompanying charge reorganization previously illustrated.^{14,18} Density is removed from the antibonding (nonbonded) regions and the immediate vicinities of both nuclei, where V is maximally negative and T is maximally positive, and accumulated in a diffuse distribution in the binding region resulting in relaxation of the gradients in ρ . Thus V is increased and T is

decreased and an attractive Feynman force acts on the nuclei. This, as pointed out by Feynman, is the origin of the initial $1/R^6$ long-range attraction between neutral atoms.¹³

At $R = R_i$, ($R_i \sim 2$ au for H_2 and ~ 2.5 au for N_2 , for example), the signs of the derivatives are again uniquely determined, $dT/dR < 0$ and $dV/dR > 0$, and *T must increase and V decrease upon further approach of the atoms*, changes that actually take effect for $R > R_i$. Recall that $F(R)$ attains its maximum attractive value at $R = R_i$ and thus the charge reorganization in this range of R is dominated by the accumulation of density in the binding region, a process that continues for $R < R_i$, leading to $\Delta T > 0$ and $\Delta V < 0$, as required by the virial theorem at $R = R_e$.

Thus for $\Delta T < -\Delta E$, as found for $R > R_e$, the forces are attractive and the nuclear virial is stabilizing while for $R < R_e$, $\Delta T > -\Delta E$, the Feynman forces are repulsive and the nuclear contribution to the virial eqn (5), is positive and destabilizing. The virial theorem and its consequences apply equally to each individual atom in a molecule because of the corresponding atomic statement of the theorem,¹⁴

$$2T(A) = -V(A) \quad (8)$$

The virial theorem yields a unified view of bonding, one that relates the change in E to the changes in the kinetic and potential energies and to the forces exerted on the nuclei over the entire range of internuclear separations: $T(R)$, $V(R)$ and $F(R)$ are all inter-determined, *the behaviour of each being an inescapable consequence of the others*. Statements^{21,22} to the effect that the Feynman force theorem offers no information regarding dV/dR and dT/dR , are at variance with the unified picture of bonding afforded by the virial theorem.

As noted above, the creation of attractive Feynman forces on the nuclei on the initial approach of two neutral atoms is a result of tightly bound density being transferred from the region of each nucleus to a diffuse distribution in the binding region, causing the potential energy to initially increase and the kinetic energy to decrease. Thus the curve for $V(R)$ versus R is similar to the curve shown for corresponding behaviour of the atomic Ehrenfest force $\mathcal{F}(C)$; both functions attain their maximum value for large R and both change sign and become attractive at values of R in excess of R_e . Clearly $\mathcal{F}(A)$ parallels the potential energy of interaction between the atoms. The question arises as to whether $\mathcal{F}(A)$ will continue to become increasingly more attractive as R decreases, or whether it will eventually reflect the repulsion generally associated with the merging of 'inner shell electrons'. In preparation to answering this question, the definition of atomic shell structure provided by the Laplacian of the electron density is briefly summarized.

3. Laplacian representation of shell structure

The Laplacian of the electron density has the property of showing where electronic charge is locally concentrated, where $\nabla^2\rho < 0$, and locally depleted, $\nabla^2\rho > 0$. The topology of the Laplacian of the density has been shown to provide an empirical mapping of the concepts of bonded and nonbonded electron pairs embodied in the Lewis model and in the VSEPR model of molecular geometry in terms of the number and arrangement of its local maxima, the local charge concentrations.²³ It has since been demonstrated that Laplacian of the electron density exhibits a structural homeomorphism with the Laplacian of the conditional pair density,²⁴ whose maxima denote the positions where the pair density is concentrated for a given location of a 'localized' electron pair, a pair approaching the limit of total localization of the density of the Fermi hole.²⁵ Thus the Laplacian of the electron density recovers the essential spatial pairing of the electrons in real space as determined in the six-dimensional space of the pair density.

The Laplacian is known to give physical expression to atomic shell structure in terms of pairs of alternating shells of charge concentration and charge depletion, the innermost 'shell' of charge concentration being a spike-like concentration at the

nucleus.^{26,27} It is important to note for the present discussion, that the shell structures exhibited by the two Laplacians, of the density and of the conditional pair density, are essentially isomorphic and the atomic shell structure exhibited by the Laplacian of the density is a faithful representation of the real-space structure imposed by the six-dimensional electron pair density.²⁴

The shell structure defined by the Laplacian duplicates that anticipated on the basis of equating the number of shells to the principal quantum number n for atoms up to Xe, with the exception of transition metal atoms and including neighbouring metalloids.^{28,29} For the transition metal atoms and metalloids (up to and including Ge in the fourth row) only $n - 1$ such alternating pairs of shells are found. The 'missing' shell was interpreted by some²⁹ as a failure of the Laplacian, an interpretation dispelled by the demonstrated homeomorphism of $\nabla^2\rho(\mathbf{r})$ with that of the conditional pair density.

Maps of the Laplacian of the density are employed to provide a pictorial representation of the approach and merging of atomic shells as atoms approach one another. This topology is complemented with that of the density itself, the evolution of the number and type of its critical points (CP) in the internuclear region as R decreases from infinity to the UA limit, providing a succinct summary of the topology of the density. Costales *et al.*³⁰ have considered the behaviour of the density and its Laplacian as a function of R for a representative set of diatomic molecules down to distances of 0.6 au, in preparation of the study of the density for systems under pressure, their study adding to the evidence that the density and its Laplacian at a bond CP exhibit a clear exponential behaviour if expressed as a function of the internuclear separation.^{28,31,32} They demonstrated a universal change in bonding regimes, as determined by the sign of the Laplacian at the bond CP, from closed-shell for large R ($\nabla^2\rho_b > 0$) to shared ($\nabla^2\rho_b < 0$), up to separations where the inner shells begin to interact and the cycle is repeated. The behaviour of ρ_b and $\nabla^2\rho_b$ in the range $\infty < R < R_e$ has previously been studied for molecules covering the range from shared to closed-shell interactions.¹⁹ The present work complements the earlier studies, extending them to the UA limit and correlating the changes in the topological properties of ρ and its shell structure with the behaviour of the kinetic and potential energies and the Feynman forces through the virial theorem.

4. Approach to the united atom limit: $0 < R \leq R_e$

4.1 UA approach in He₂

The He₂ molecule is calculated to have well depth of approximately 11 K (0.02 kcal mol⁻¹) at $R = 5.6$ au.^{33,34} The present calculations focus on the approach of the atoms to the UA limit. The changing topology of the density is depicted in Fig. 2 in terms of the total density and profiles along the internuclear axis. As anticipated, $\rho(\mathbf{r}_c)$, the density at the central (3, -1) CP, undergoes an exponential increase as R is decreased, from its value of 5×10^{-4} au at $R = 6.0$ au to a value of 22.8 au at $R = 0.09$ au. A further decrease in R to 0.08 au causes the central (3, -1) CP to bifurcate into a (3, -3) central maximum with a value of 23.9 au—a non-nuclear attractor (NNA)-bordered by two (3, -1) CPs. The central maximum in the density surpasses the nuclear maxima by $R = 0.08$ au, the first topological evidence of the approach to the UA limit. The electron population of the non-nuclear attractor (NNA) is 2.38 e at $R = 0.05$ au. For some value of R less than 0.05 au, each nuclear maximum in ρ is annihilated by coalescing with its neighbouring (3, -1) CP and the density exhibits a single maximum characteristic of the UA limit.

The value of the Laplacian at the (3, -1) CP at the mid point of the internuclear axis, $\nabla^2\rho(\mathbf{r}_c)$, is positive for values of $R > 1.2$ au, as anticipated for a closed-shell interaction, having a value of +0.0031 au at R_e and increasing to a maximum value of 1.58 au at $R \sim 1.5$ au. For all values of R in excess of this, the Laplacian exhibits a

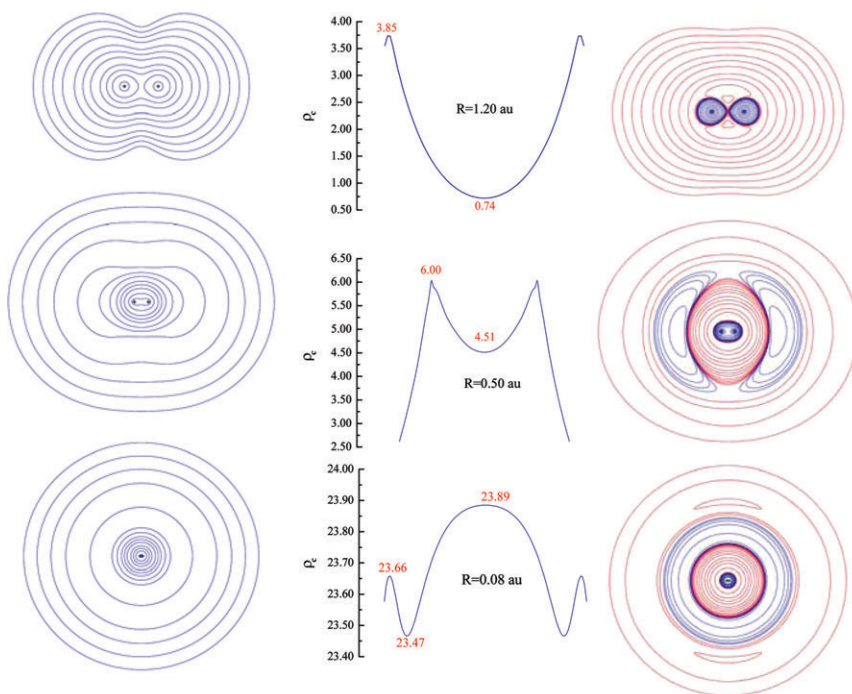


Fig. 2 Progressive changes in the density $\rho(r)$, in contour plots and as internuclear profiles (in au), together with the accompanying changes in the Laplacian distribution, for the approach of two He atoms to the UA limit. The outer contour value is 0.001 au and the remaining contours increase in value in the order 2×10^{-4} , 4×10^{-4} , 8×10^{-4} au with n beginning at -3 and increasing in steps of unity. The same contour values for both positive and negative values are used in the Laplacian maps beginning with $n = -3$ about a zero contour. The same contours are used in all density maps. Regions of charge concentration, $\nabla^2\rho < 0$, are in blue, regions of charge depletion $\nabla^2\rho > 0$ in red.

single encompassing outer shell of charge depletion (CD), where $\nabla^2\rho > 0$, and two separate nuclear centred shells of charge concentration (CC), where $\nabla^2\rho < 0$.

The point at which the two inner shells of CC come into contact is readily determined by noting the value of R at which $\nabla^2\rho(r_c) = 0$ and the Laplacian changes sign. This occurs for R slightly less than 1.2 au, Fig. 2 and one might anticipate that this value of R will indicate a possible change in the character of the Ehrenfest force, if indeed closed-shell repulsion is a physical effect. From this point on, the inner shells of CC form a contiguous region of charge concentration and the initially closed-shell interaction assumes the characteristics of a shared interaction and $\nabla^2\rho(r_c)$ becomes increasingly negative, equaling $-\infty$ at $R = 0$.

The united atom (UA) Be has two quantum shells and following on the merging of the two inner shells of CC, a second, outer shell of CC appears with local maxima in each of the antibinding regions, as illustrated in Fig. 2 for $R = 0.5$ au. These regions have merged into a nuclear centered shell at $R = 0.1$ au, as illustrated for $R = 0.08$ au, and the structure is homeomorphic with that of the UA. The creation of a NNA followed by the annihilation of the nuclear maxima is characteristic of the UA approach for a homonuclear system.

4.2 UA approach in LiF

LiF is calculated to have an energy minimum at $R_e = 3.016$ (2.96) au and a well depth of 5.68 (6.00) eV with the experimental values bracketed. The bonding is ionic

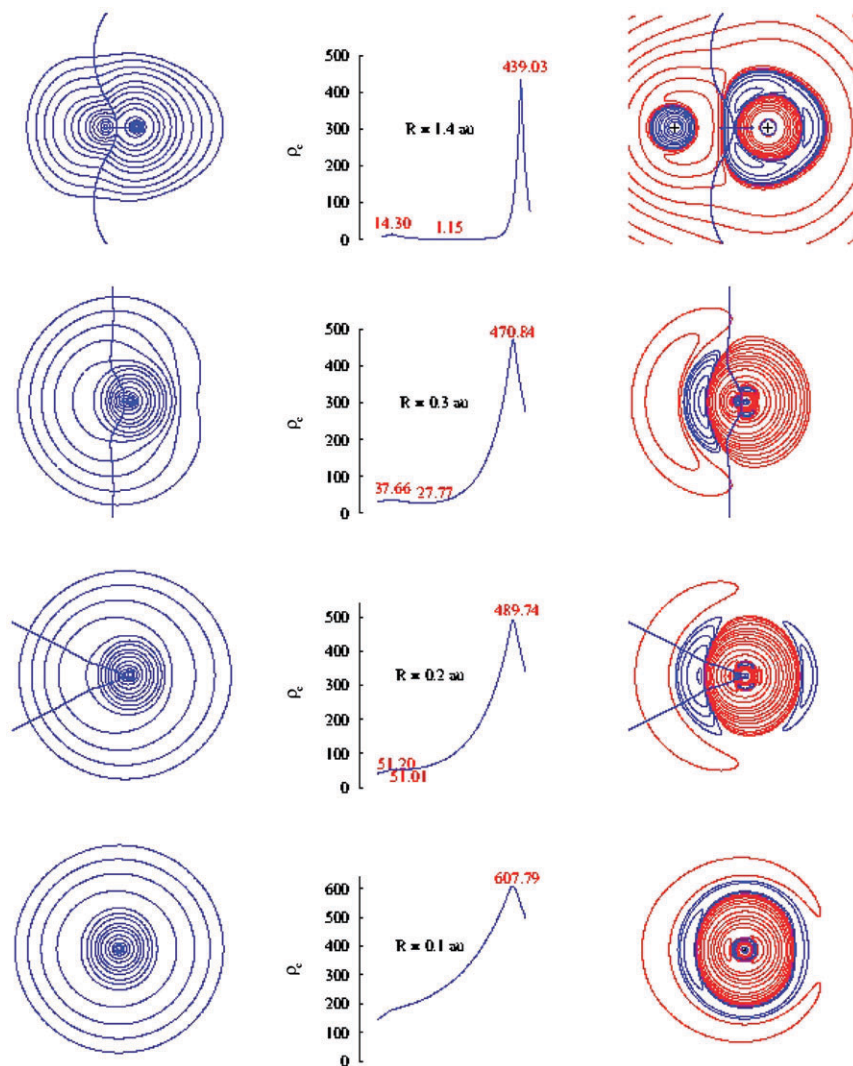


Fig. 3 Similar diagram to that in Fig. 2 for the approach of the atoms to the UA limit in LiF.

with atomic charges of ± 0.94 e with closed-shell characteristics, $\rho_b = 0.072$ au and $\nabla^2\rho_b = +0.609$ au. Fig. 3 displays the density, its axial profile and the Laplacian for approach to the UA limit, a Mg atom in its 1S ground state. Fig. 4 displays the evolution of the Laplacian distribution in terms of the zero envelopes that define the boundaries of the shells. The shell structure for $R = 1.4$ is that found at R_c with F exhibiting three nodal surfaces for two shells and Li exhibiting a single node defining the inner shell CC. The approach of the Li core causes a polarization of the initially spherical valence shell CC (VSCC) on F into a toroidal CC that encircles the axis, as evident in the envelope display for $R = 0.45$ au and the contour plot for $R = 0.3$ au.

The value of $\rho(r_c)$ increases exponentially, equaling 51 au at $R = 0.20$ where its value is 0.2 au less than the nuclear maximum at Li. The bond CP vanishes for a further decrease in R and at $R = 0.1$ au only the required cusp remains at the position of the Li nucleus. This is the topological behaviour obtained for the approach to UA limit for a heteronuclear molecule. It is the topology observed

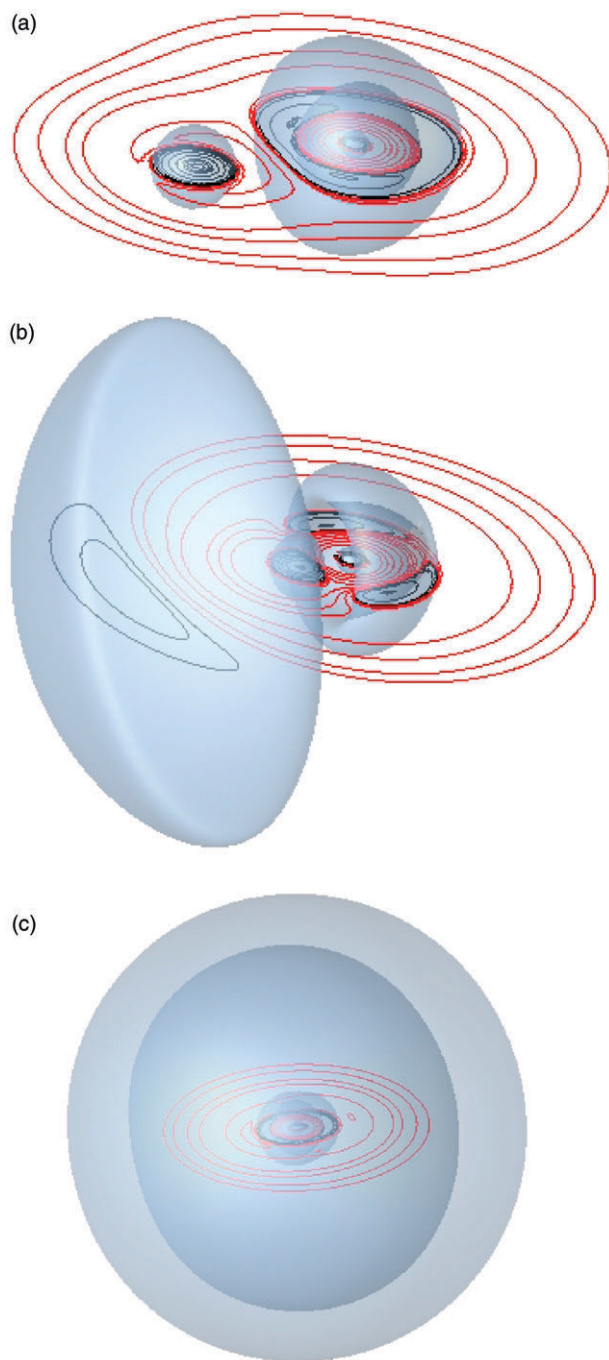


Fig. 4 Envelope displays of the Laplacian distribution for decreasing R values in LiF. The zero envelopes used in this figure separate the regions of charge concentration (blue) from charge depletion (red). Values of R in au are: 1.40 in (a), 0.45 in (b) and 0.10 in (c).

for the ground state of FH^+ that approaches the UA limit in its equilibrium geometry, a result of hydrogen not possessing a core density.³⁵ The value of $\nabla^2\rho(r_c)$ attains its largest value of 487 au at $R = 0.45$ au beyond which it decreases

precipitously becoming negative at $R \sim 0.33$ au, the point at which the bond CP enters the inner shell of CC on Li and the sign change is not a result of the merging of the inner cores, but because of the migration of the bond CP into the core of Li. The inner shell cores merge between $R = 0.25$ and 0.20 au preceding slightly the bifurcation point in the density. The third quantum shell first appears in the nonbonded region of Li as is apparent at $R = 0.3$ au. There is but a single nuclear maximum for $R < 0.2$ au and the topology is that of the UA with the third quantum shell now encompassing the entire molecule, as displayed for $R = 0.1$ au in Fig. 3 and 4. At this separation, the nuclear maximum at F has a value of 608 au, compared to the value of 1059 au for the Mg atom, the UA limit.

The energy density at the bond CP H_b which is positive for an ionic interaction changes sign before $\nabla^2\rho_b(r_c)$ does, becoming negative by $R = 2.0$ au and decreasing to -845.5 au at $R = 0.3$ au just before the point of bifurcation and the disappearance of the bond CP. As in the case of He_2 , the initially closed-shell interaction assumes the characteristics of a shared interaction as density is accumulated in the internuclear region. An interesting feature displayed in the density maps is the relative shift in the position of the bond CP towards the F nucleus as R is decreased, the ratio $r_b(\text{Li})/R$ increasing from 0.39 at R_c to 0.71 at $R = 0.45$. This has the effect of increasing the electronic population of Li such that its atomic charge decreases from $+0.94$ e to -1.16 e at $R = 0.45$ au. The charge transfer is evident in the initially paraboloid interatomic surface characteristic of an ionic interaction being replaced at $R = 1.4$ au with a surface that reflects the transfer of density to the Li atom reducing its charge from $+0.9$ to $+0.5$. A further decrease in R to 0.30 au, just before the point of bifurcation, the point where $\nabla^2\rho(r_c)$ becomes negative as the two inner shells nearly touch, the $r_b(\text{Li})/R$ ratio decreases to 0.25 and $q(\text{Li})$ increases to -0.70 e.

4.3 UA approach in N_2

The ground state ($^1\Sigma_g^+$) N_2 is calculated to have $R_c = 2.066$ (2.074) au and $D_e = 9.243$ (9.892) eV. The UA limit is the lowest energy ^1D state of Si. The interaction has the characteristics (in au) of a shared interaction: $\rho_b = 0.720$, $\nabla^2\rho_b = -3.453$ and $H_b = -1.513$. The value of $\rho(r_c)$ undergoes the anticipated increase with decreasing R , with the formation of a NNA at $R \sim 1.9$ au. The new central maximum is not pronounced, its value of 1.160 au at $R = 1.7$ au exceeding the values of the neighbouring $(3, -1)$ CPs by only 0.005 au and having vanished by coalescence with these same CPs by $R = 1.38$ au. The central bonded CC in the Laplacian distribution present in the equilibrium distribution and characteristic of a shared interaction becomes increasingly pinched and is at the point of bifurcation at $R = 1.05$ au, Fig. 5. A further decrease in R results in $\nabla^2\rho(r_c) > 0$ and the formation of a local minimum, with the remnants of the bonded CC forming a torus encircling the axis. The third quantum shell is evident at $R = 0.65$ au, its appearance being dominated by two nonbonded CCs, Fig. 5. The Laplacian $\nabla^2\rho(r_c)$ becomes negative again at $R \sim 0.25$ au indicating the coalescence of the two inner cores of CC on the nitrogen nuclei. Continued decrease in R causes an increasing accumulation of density at the bond CP, and by $R = 0.03$ au the Laplacian approaches the UA limit of the Si atom. The final bifurcation of the density to yield a single central maximum occurs between $R = 0.008$ au for which $\rho(r_c) = 1462.73$ au and $R = 0.007$ au, for which only a central maximum is found with $\rho(r_c) = 1485$ au, compared to $\rho(0) = 1742$ au for the Si atom.

4.4 UA approach in CO

Carbon monoxide in its $^1\Sigma^+$ ground state is calculated to have $R_c = 2.13$ (2.138) au and $D_e = 10.78$ (11.18) eV with the characteristics (in au) of a polar interaction: $\rho_b = 0.498$, $\nabla^2\rho_b = +0.732$, $H_b = -0.928$ au and with atomic charges of ± 1.22 .

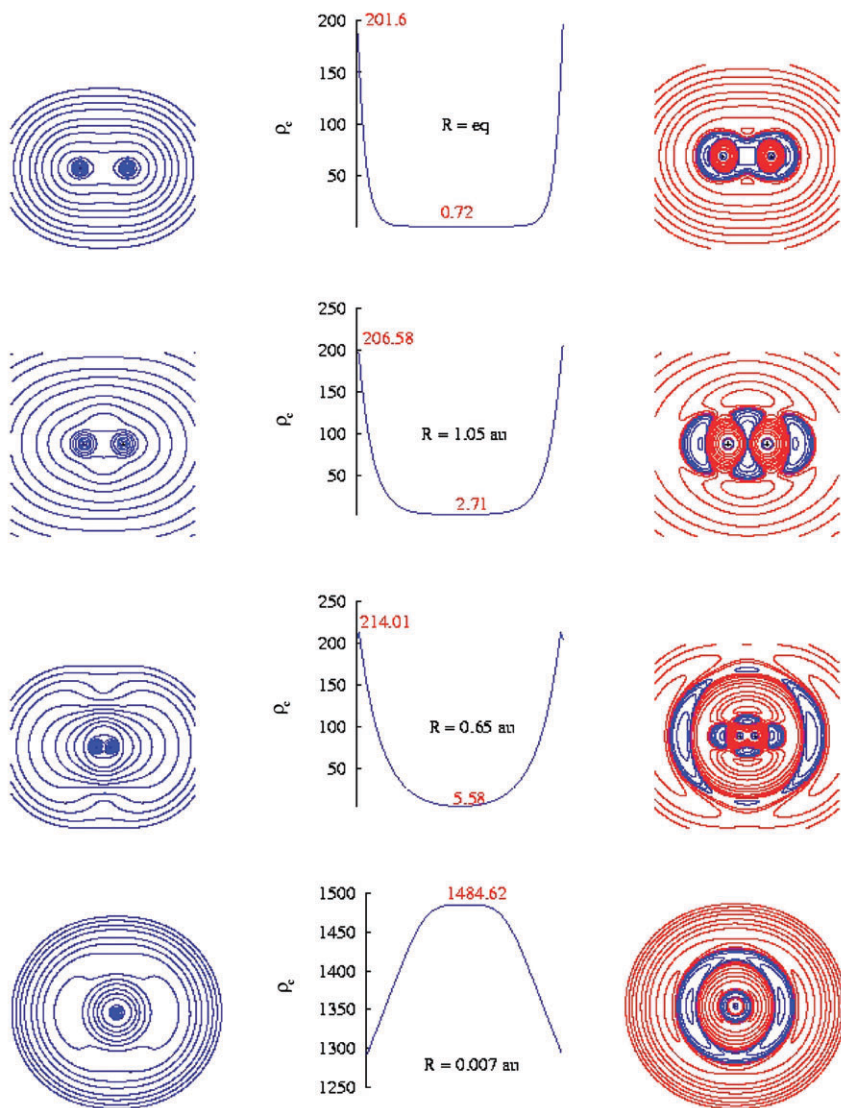


Fig. 5 Similar diagram to that in Fig. 2 for the approach of the atoms to the UA limit in N_2 .

Fig. 6 displays the density, its axial profile and the Laplacian for approach to the same UA limit as for N_2 , the 1D state of Si. The bond CP in the equilibrium distribution for $R = 2.13$ au occurs within the steeply rising region of charge removal within the C basin, close to the point where $\nabla^2\rho_b$ changes sign, a consequence of the charge transfer to oxygen resulting in the formation of a bonded CC within the O basin. There is a progressive increase in the density at the bond CP and at each nucleus, with the value of $\rho(r_c)$ approaching the value at the C nucleus, the nuclear bifurcation resulting in the disappearance in the nuclear maximum at C occurring just past the $R = 0.05$ au. Only a single nuclear maximum remains for smaller R values, the topological transformation to the UA limit paralleling that found for LiF. The nuclear bifurcation for Li occurs at a larger value of $R = 0.20$ au reflecting the greater disparity in nuclear charges found in LiF. The density at the

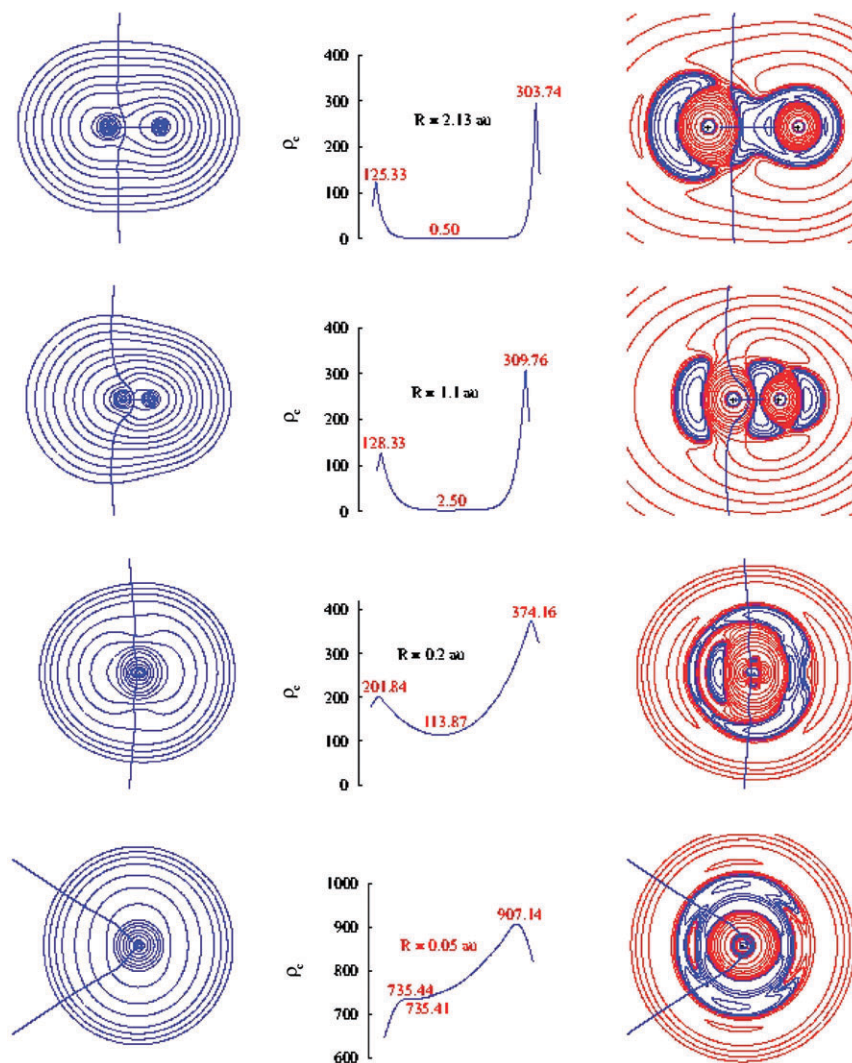


Fig. 6 Similar diagram to that in Fig. 2 for the approach of the atoms to the UA limit in CO.

oxygen nucleus at $R = 0.01$ au equals 1,518 au compared to $\rho(0) = 1,742$ au for the Si UA. The charge on C increases to a maximum value of $+1.6$ e at $R = 1.20$ au.

Both C and O exhibit valence shell charge concentrations with the nonbonded CC on carbon being particularly pronounced, a CC that is reduced in magnitude as R is decreased. At $R = 1.1$ au the bonded CC on oxygen is transformed into a torus of CC encircling the axis and the pattern within the oxygen VSCC on oxygen is similar to that found for fluorine in LiF at $R = 1.4$ au, Fig. 4. The value of $\nabla^2\rho(r_c)$ becomes increasingly positive as R decreases, attaining a value of 2200 au for $R \sim 0.35$ au following which there is steep decline and $\nabla^2\rho(r_c)$ becomes negative as the inner cores of CC merge at $R \sim 0.25$ au. This merging of the shells is accompanied by the appearance of the third quantum shell characteristic of the Si atom. At $R = 0.05$ au the value of ρ_c is only 0.03 au less than the value of ρ at the C nucleus and for a further decrease in R , the two critical points merge and the density exhibits but a single maximum. Thus the density distributions of LiF and CO exhibit the same topological behaviour as a function of R .

4.5 Mechanics of atomic interactions, $R_e \rightarrow$ UA limit

The diagrams in Fig. 7 display the behaviour of the total energy E , the electronic kinetic energy T , the atomic Ehrenfest force $\mathcal{F}(A)$ and the total electronic energy $H_e = V_{en} + V_{ee} + T$, all as functions of R , down to the UA limit of the energy, beginning in the neighbourhood of R_e for LiF, N_2^{36} and CO and at $R = 1.0$ au for He_2 . The energies, E , T and H_e and the force $\mathcal{F}(A)$ behave similarly for all four molecules. The total energy increases exponentially for separations less than 0.5 au for LiF, N_2 and CO and for $R < 0.2$ au for He_2 . In every case, the electronic energy H_e undergoes a monotonic decrease to the UA limit: $E(^1S; Be) = -14.6609$ for He_2 ; $E(^1S; Mg) = -199.7304$ au for LiF and $E(^1D; Si) = -288.9683$ au for N_2 and CO. While the kinetic energy does increase as the atoms are brought together, its limiting value is constrained by the virial theorem to equal to the negative of the UA energy.

The decrease in H_e to the UA limit is a result of the electron–nuclear attractive energy overwhelming the electron–electron repulsion and the increasing kinetic energy. Since $E = H_e + V_{nn}$, the increase in E is clearly the result of the increase in V_{nn} for close-approach of atoms. One notes that as required by the virial theorem, eqn (7), T exceeds $-E$ in the repulsive region, a consequence of the nuclear virial

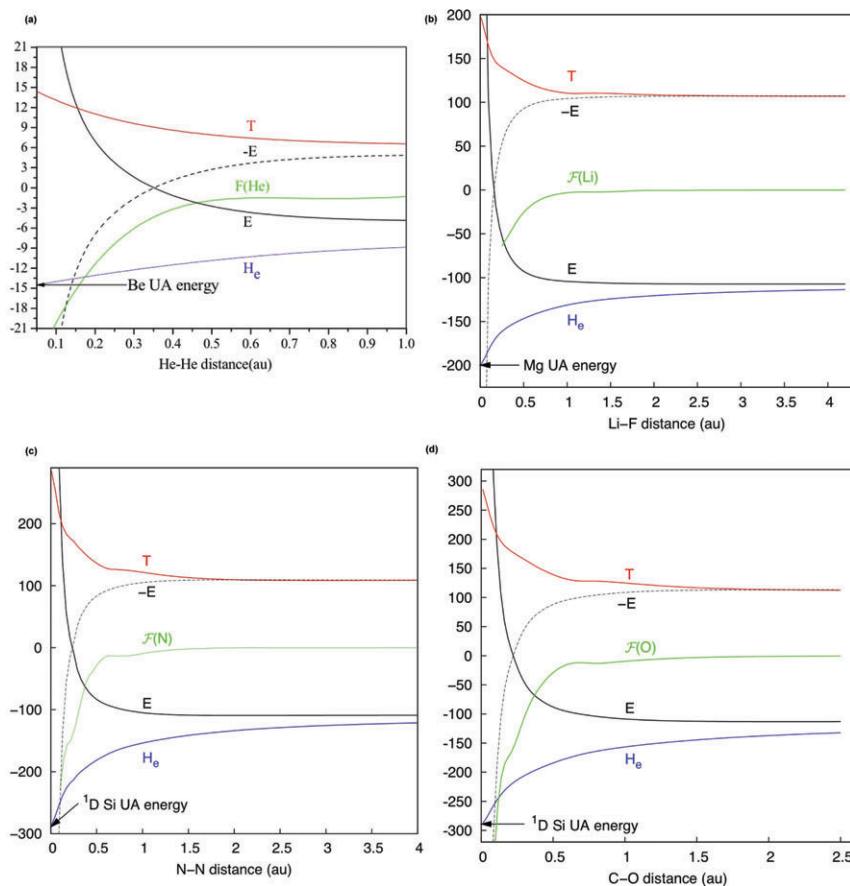


Fig. 7 The variations in E , T , the electronic energy H_e and the Ehrenfest force $\mathcal{F}(A)$, from $\sim R_e$ to the UA limit for He_2 , LiF, N_2 and CO. The separation between $-E$ and T is a measure of the contribution virial of the Feynman forces to the total molecular virial. The $-E$ and T curves for He_2 exhibit the same monotonic behaviour out to 6 au and have effectively merged by 3.5 au.

RdE/dR being destabilizing for repulsive forces. This behaviour is brought to the fore by comparing T with the dashed curve for $-E$, Fig. 7. The gap between T and $-E$, one that increases with decreasing R , is a measure of the virial of the nuclear repulsive force. Thus while T does increase as R is decreased, its contribution does not dominate the electronic contributions to the energy as shown by H_e decreasing to the UA limit. Instead, it is the nuclear force of repulsion that is responsible for the exponential increase in E for close approach of the atoms.

One might have thought that $\mathcal{F}(A)$, the Ehrenfest force acting on the atoms, could become repulsive for approach of the atoms for $R \ll R_e$, having in the back of one's mind the model of 'Pauli repulsions acting between closed-shell atoms'. The repulsion of the electrons on A by those on B could conceivably override the attraction of the density on A by the nucleus of B once the atomic cores defined by the inner shells of charge concentration are brought into contact. The Laplacian maps show that the inner shells of CC merge at $R \sim 1.2$ au for He_2 and at $R \sim 0.25$ au for LiF, N_2 and CO. $\mathcal{F}(A)$ does exhibit a slight shoulder for LiF, CO and N_2 in the region of $R = 0.25$ au as well as a very slight dip in the region of 1.2 for He_2 . Aside from these small variations which may be artifacts of the numerical integrations, the overriding behaviour of $\mathcal{F}(A)$ is to exhibit a nearly continuous decrease, demonstrating that the nuclear–electron attractive forces dominate the electronic repulsions down to the point where the interatomic surface vanishes and $\mathcal{F}(A)$, like H_e , is dominated by the electron–nuclear force of attraction, resulting from the continuous accumulation of density between the nuclei.

5. Discussion

In a bound molecular state, the nuclei of bonded atoms are linked by a line along which the electron density is a maximum with respect to any neighbouring line; they are linked by a *bond path*. A bond path meets all of the physical requirements set by the Ehrenfest, Feynman and virial theorems that the atoms be bonded to one another;⁷ the two atoms experience an attractive Ehrenfest force drawing their atomic basins together: no Feynman force, neither attractive nor repulsive, acts on the nuclei because of the balancing of the repulsive and attractive forces by the accumulation of electron density in the binding region: this same accumulation leads to a lowering of the electron–nuclear potential energy whose magnitude exceeds the increases in the electron and nuclear repulsion energies, as demanded by the virial theorem. Thus a bond path is indicative of the accumulation of density between the nuclei that is necessary for the presence of attractive Ehrenfest forces, for a balancing of the Feynman forces on the nuclei and for the decrease in energy. Its presence is both necessary and sufficient for two atoms to be bonded to one another. A bond path is mirrored by a 'virial path', a line along which the potential energy density is maximally stabilizing and the formation of the line of maximum density is associated with a local lowering in the energy.³⁷

These requirements are universal and apply to all bonding, shared (covalent), closed-shell ('non-bonded'), hydrogen bonding, di-hydrogen bonding, ionic bonding, metal–metal bonding and van der Waals bonding, that is, dispersion forces.^{14,18,19,38} The different classes of bonding differ not in their underlying physics, but rather in the manner and degree to which the electron density is accumulated in the internuclear region, the properties determined at the associated bond critical point providing a succinct summary of the physical characteristics of a bonded interaction. These include properties determined by the electron density ρ_b , its Laplacian $\nabla^2\rho_b$ and the associated ellipticity and by the appropriate energy density; the kinetic energy density G_b , the potential energy (the virial) density ν_b and the energy density $H_b = G_b + \nu_b$. Gatti has given a particularly full account of the application of QTAIM to crystals, paying particular attention to the chemical significance of bond paths for the very weak and supposedly repulsive interactions.³⁹ Coppens and Kortisanszky state that the intermolecular bond paths present in

crystals and determined by accurate X-ray diffraction experiments, are essential to the understanding of crystal structures.⁴⁰

Poater *et al.*⁴¹ claim that nonbonded interactions in molecular solids are subject to Pauli repulsions because of the impossibility of forming an 'electron pair bond' and ascribe the stability of the crystal to the presence of weak dispersion forces. Thus they claim that the individual molecules in solid benzene repel one another through the contact of their H atoms, and yet at the same time, the crystal is stabilized by dispersion forces! There are no Pauli repulsive forces as invoked by Bickelhaupt and Baerends⁴ or Poater *et al.*⁴² They arise only in calculations that first arbitrarily ignore orbital orthogonality *thereby violating the Pauli principle*, followed by its reinstatement at a latter stage.^{6,18} If the presence of the 'Pauli repulsions' does not lead to a physical repulsion, what precisely is its role in understanding the properties of matter, predicting as it does the presence of a force that has no measurable or physical consequences? The same authors argue that the finding of a bond path in 'nonbonded interactions' contradicts the orbital model of bonding. It is a travesty to claim that molecular orbital theory does not account for the bonding between closed-shell systems by insisting that one terminate the theory at the single determinant level.^{43,44}

In response to criticisms of QTAIM and its description of bonding, one need only recall that the electron density obtained in a variational calculation is the distribution that minimizes the energy for any geometry and thus the presence of bond paths represent spatial accumulations of the density that lower the energy of the system. Their properties provide a physical classification of the interactions in terms of the density, an observed property of a system that is subject to the theorems of quantum mechanics, thereby setting it apart from the approaches employed by those who would criticize it.

Physics determines whether two atoms that 'touch' are bonded or are repelling one another. As demonstrated above, the only repulsive force operative upon close approach of atoms or molecules is the Feynman force of repulsion acting on the nuclei. The Feynman force is after all, the force that is related to the gradients of the potential energy surface and hence it is measurable. Expressing the potential energy in terms of a set of ($3N - 6$) normal or internal coordinates, enables one to relate the gradient of the potential along an internuclear separation to the corresponding Feynman force, a repulsive force being the result of the nuclear force of repulsion outweighing the e-n force of attraction. Thus closed-shell atoms or molecules that 'touch' in an equilibrium geometry where no Feynman forces act on the nuclei, do not repel, but are instead bonded to one another since if they 'touch', they share an interatomic surface and their nuclei are necessarily linked by a bond path.

Acknowledgements

J. H.-T. and F. C.-G. acknowledge DGSCA-UNAM for computer resources.

References

- 1 J. C. Slater, *J. Chem. Phys.*, 1933, **1**, 687.
- 2 J. C. Slater, *Quantum Theory of Molecules and Solids. I*, McGraw-Hill Book Co. Inc., New York, 1963.
- 3 J. D. Dunitz and A. Gavezzotti, *Angew. Chem., Int. Ed.*, 2005, **44**, 1766.
- 4 F. M. Bickelhaupt and E. J. Baerends, *Angew. Chem., Int. Ed.*, 2003, **42**, 4183.
- 5 V. Pophristic and L. Goodman, *Nature*, 2001, **411**, 565.
- 6 R. F. W. Bader, *Chem.-Eur. J.*, 2006, **12**, 2896.
- 7 R. F. W. Bader, *J. Phys. Chem. A*, 1998, **102**, 7314.
- 8 J. A. Pople and M. Head-Gordon, *J. Chem. Phys.*, 1987, **87**, 5968.
- 9 T. A. Keith, Private modification of GAUSSIAN code 1992.
- 10 D. E. Woon and T. H. Dunning, Jr., *J. Chem. Phys.*, 1994, **100**, 2975.
- 11 A. J. Sadlej, *Collect. Czech. Chem. Commun.*, 1988, **53**, 1995.
- 12 A. J. Sadlej and M. Urban, *THEOCHEM*, 1991, **234**, 147.

- 13 R. P. Feynman, *Phys. Rev.*, 1939, **56**, 340.
- 14 R. F. W. Bader, *Atoms in Molecules: A Quantum Theory*, Oxford University Press, Oxford UK, 1990.
- 15 R. F. W. Bader, *Phys. Rev. B*, 1994, **49**, 13348.
- 16 R. F. W. Bader and F. De-Cai, *J. Chem. Theor. Comput.*, 2005, **1**, 403.
- 17 R. F. W. Bader, *J. Chem. Phys.*, 1980, **73**, 2871.
- 18 F. Cortés-Guzmán and R. F. W. Bader, *Coord. Chem. Rev.*, 2005, **249**, 633.
- 19 J. Hernández-Trujillo and R. F. W. Bader, *J. Phys. Chem. A*, 2000, **104**, 1779.
- 20 R. F. W. Bader, in *The Force Concept in Chemistry*, ed. B. M. Deb, Van Nostrand Reinhold Co., New York, 1981, pp. 39–136.
- 21 K. Ruedenberg, *Rev. Mod. Phys.*, 1962, **34**, 326.
- 22 M. J. Feinberg and K. Ruedenberg, *J. Chem. Phys.*, 1971, **54**, 1495.
- 23 R. F. W. Bader, P. J. MacDougall and C. D. H. Lau, *J. Am. Chem. Soc.*, 1984, **106**, 1594.
- 24 R. F. W. Bader and G. L. Heard, *J. Chem. Phys.*, 1999, **111**, 8789.
- 25 R. F. W. Bader and M. E. Stephens, *J. Am. Chem. Soc.*, 1975, **97**, 7391.
- 26 R. F. W. Bader and P. M. Beddall, *J. Chem. Phys.*, 1972, **56**, 3320.
- 27 R. F. W. Bader and H. Essén, *J. Chem. Phys.*, 1984, **80**, 1943.
- 28 Z. Sijhi and R. J. Boyd, *J. Chem. Phys.*, 1988, **88**, 4375.
- 29 R. P. Sagar, A. C. T. Ku and V. H. Smith, *J. Chem. Phys.*, 1988, **88**, 4367.
- 30 A. Costales, M. A. Blanco, A. M. Pendás, P. Mori-Sánchez and V. Luaña, *J. Phys. Chem. A*, 2004, **108**, 2794.
- 31 R. J. Boyd and S. L. Boyd, *J. Am. Chem. Soc.*, 1992, **114**, 1652.
- 32 M. Pendás, M. A. Blanco, A. Costales, P. Mori-Sánchez and V. Luaña, *Phys. Rev. Lett.*, 1999, **83**, 1930.
- 33 J. B. Anderson, *J. Chem. Phys.*, 2004, **120**, 9886.
- 34 T. van Mourik, R. J. Vos, J. H. van Lenthe and F. B. van Duijneveldt, *Int. J. Quantum Chem.*, 1997, **63**, 805.
- 35 R. F. W. Bader, Y. Tal, S. G. Anderson and T. T. Nguyen-Dang, *Isr. J. Chem.*, 1980, **19**, 2871.
- 36 The Ehrenfest force $F(N)$ plotted in Fig. 7 for the N_2 molecule in the region of the NNA is the force exerted on a N atom acting across the surface it shares with the NNA. This surface defines a nitrogen atom, call it N1 and the group $NNA + N_2$. The Ehrenfest force acting on the NNA is zero because the forces acting on its two bounding surfaces are equal and opposite.
- 37 T. A. Keith, R. F. W. Bader and Y. Aray, *Int. J. Quantum Chem.*, 1996, **57**, 183.
- 38 R. F. W. Bader, J. Hernández-Trujillo and F. Cortés-Guzmán, *J. Comput. Chem.*, 2006, in press.
- 39 C. Gatti, *Z. Kristallogr.*, 2005, **220**, 399.
- 40 T. S. Koritsanszky and P. Coppens, *Chem. Rev.*, 2001, **101**, 1583.
- 41 J. Poater, M. Solá and F. M. Bickelhaupt, *Chem.–Eur. J.*, 2006, **12**, 2902.
- 42 J. Poater, M. Solá and F. M. Bickelhaupt, *Chem.–Eur. J.*, 2006, **12**, 2889.
- 43 The bound helium dimer has been observed experimentally and reported in the paper “The weakest bond: Experimental observation of helium dimer”⁴⁴.
- 44 F. Luo, G. C. McBane, G. Kim, C. F. Giese and R. Gentry, *J. Chem. Phys.*, 1993, **98**, 3564.